Conditions for primitive-lattice-vector-direction equal contrasts in four-beam-interference lithography

Justin L. Stay and Thomas K. Gaylord*

School of Electrical and Computer Engineering, Georgia Institute of Technology, 777 Atlantic Drive. N.W., Atlanta, Georgia 30332-0250, USA

*Corresponding author: tgaylord@ece.gatech.edu

Received 9 April 2009; accepted 28 July 2009;
posted 4 August 2009 (Doc. ID 109906); published 19 August 2009

Four distinct *conditions for primitive-lattice-vector-direction equal contrasts* in four-beam interference are introduced and described. By maximizing the absolute contrast subject to an equal contrast condition, lithographically useful interference patterns are found. Each condition is described in terms of the corresponding constraints on the plane wave wave vectors, polarizations, and intensities. The resulting locations of global intensity maxima, minima, and saddle points are presented. Subordinate conditions for unity absolute contrast are also developed. Three lattices are treated for each condition: simple cubic, face-centered cubic, and body-centered cubic. © 2009 Optical Society of America

OCIS codes: 050.1950, 050.5298, 110.3960, 110.4235, 220.3740, 350.4238.

1. Introduction

Photonic crystal technology offers the potential of lossless control of the propagation of light at microelectronic and nanoelectronic size scales [1]. This technology may be instrumental in producing the first truly dense integrated photonic circuits and systems. Numerous important physical characteristics have already been demonstrated. These phenomena include the photonic bandgap [1], the superprism effect [2–4], negative refraction [5,6], and negative diffraction [7–9]. Individual components that have been demonstrated include waveguides [10,11], resonators [12–15], filters [15–18], waveguide couplers [19–22], directional couplers [23], demultiplexers [24], antennas [25], switches [26], and sensors [27]. There are a number of techniques currently used to fabricate photonic crystal structures and devices. Some of these are two-photon polymerization [28,29], focused-ion-beam etching [30], self-assembly [31–33], optical lithography [34–36], and e-beam lithography [35,37–39]. A relatively new technique for defining the photoresist mask and polymer templates used to construct photonic crystal structures is multibeam-interference lithography (MBIL) [40–42]. By interfering two or more coherent beams of light, periodic interference patterns can be created and are used to expose and define photosensitive materials to be used as etching masks or templates.

Previously, specific configurations of wave vectors were presented that produce interference patterns with the symmetry of all 14 three-dimensional Bravais lattices through the interference of four noncoplanar beams [43,44]. To produce a lithographically useful pattern, Cai *et al.* [44,45] introduced a concept of *uniform contrast* defined by two requirements: (1) contrast of the interference terms should be the same for multiple primitive lattice directions and (2) the absolute contrast should be as large as possible. Within four-beam interference, constraints on the intensities and polarizations of the individual beams have been given to satisfy the uniform contrast condition. However, in the literature there is no complete treatment of uniform contrast itself.

Here we introduce four *conditions for primitive-lattice-vector-direction equal contrasts* to describe the contrast in four-beam interference for producing lithographically useful interference patterns. A brief description of multibeam interference is given as a

0003-6935/09/244801-13$15.00/0

basis for the subsequent discussion of four-beam interference. The concept of uniform contrast is also described. The new nomenclature, *conditions for primitive-lattice-vector-direction equal contrasts*, and a symbolic designation $C_n^{(m)}$ are introduced to provide a definitive description of the resulting interference patterns. For each *condition for primitive-lattice-vector-direction equal contrasts*, a thorough mathematical description is given including the required constraints on the plane wave parameters, the resulting locations of the maxima, minima, and saddle points within the unit cell of the periodic interference pattern, and subordinate conditions for maximum absolute contrast. Within each *condition for primitive-lattice-vector-direction equal contrasts*, three lattices are treated (simple cubic, face-centered cubic, and body-centered cubic) with tables presenting the plane wave parameters and the maximum absolute contrast for each case.

2. Multibeam Interference

The time-average electric field intensity that is due to the interference of N linearly polarized, monochromatic plane waves can be expressed as

$$I_T(\mathbf{r}) = I_0\left(1 + \sum_{i=1}^{N}\sum_{j>i}^{N} V_{ij}\cos(\mathbf{G}_{ji}\cdot\mathbf{r} + \phi_i - \phi_j)\right), \quad (1)$$

where the DC intensity term (I_0), interference coefficients (V_{ij}), polarization efficiency factors (e_{ij}), and spatial cosine wave vectors ($\mathbf{G}_{ji}$) are given by

$$I_0 = \frac{1}{2}\sum_{k=1}^{N} E_k^2, \qquad V_{ij} = \frac{E_i E_j e_{ij}}{I_0},$$
$$e_{ij} = \hat{\mathbf{e}}_i\cdot\hat{\mathbf{e}}_j, \qquad \mathbf{G}_{ji} = \mathbf{k}_j - \mathbf{k}_i, \quad (2)$$

respectively. The terms E_i, $\hat{\mathbf{e}}_i$, $\mathbf{k}_i$, and ϕ_i are the electric field amplitude, polarization vector, wave vector, and initial phase, respectively, of the ith plane wave. For this analysis, the initial phases of the interfering beams are set to zero ($\phi_i = 0$). This constraint guarantees that a set of global intensity extrema (maxima or minima) are located at the lattice points whose origin is at $\mathbf{r} = 0$. Nonzero initial phases merely translate the locations of these intensity extrema.

3. Four-Beam Interference

In general, the interference of four linearly polarized, monochromatic planes waves will produce a three-dimensional, periodic interference pattern. The primitive basis vectors **a**, **b**, and **c** are used to define the translational symmetry of the desired interference pattern. The corresponding reciprocal lattice vectors **A**, **B**, and **C** are expressed as

$$\mathbf{A} = 2\pi\frac{\mathbf{b}\times\mathbf{c}}{\mathbf{a}\cdot\mathbf{b}\times\mathbf{c}}, \qquad \mathbf{B} = 2\pi\frac{\mathbf{c}\times\mathbf{a}}{\mathbf{a}\cdot\mathbf{b}\times\mathbf{c}},$$
$$\mathbf{C} = 2\pi\frac{\mathbf{a}\times\mathbf{b}}{\mathbf{a}\cdot\mathbf{b}\times\mathbf{c}}. \quad (3)$$

A set of four wave vectors that will produce an interference pattern with the translational symmetry given by **a**, **b**, and **c** is found by locating the circumcenter (**P**) of a pyramid (tetrahedron) defined in terms of the three reciprocal lattice vectors **A**, **B**, and **C** as

$$\mathbf{P} = \frac{1}{2}\frac{|\mathbf{A}|^2(\mathbf{B}\times\mathbf{C}) + |\mathbf{B}|^2(\mathbf{C}\times\mathbf{A}) + |\mathbf{C}|^2(\mathbf{A}\times\mathbf{B})}{\mathbf{A}\cdot\mathbf{B}\times\mathbf{C}}. \quad (4)$$

The four recording wave vectors are then given by

$$\mathbf{k}_1 = \mathbf{P}, \qquad \mathbf{k}_2 = \mathbf{P} - \mathbf{A},$$
$$\mathbf{k}_3 = \mathbf{P} - \mathbf{B}, \quad \mathbf{k}_4 = \mathbf{P} - \mathbf{C}. \quad (5)$$

Unlike the three-beam case [46], the choice of the primitive basis vectors determines the wavelength required to produce the desired interference pattern. The recording wavelength needed has a magnitude of $\lambda = 2\pi/|\mathbf{P}|$. Given this methodology, it is clear that different sets of primitive basis vectors that define the same translational symmetry will produce different sets of recording wave vectors. While the translation symmetry of each will be identical, the locations of symmetry elements and stationary points within the interference pattern will differ.

Equation (1) can be written in the case of four-beam interference as

$$I_T = I_0[1 + V_{12}\cos(\mathbf{G}_{21}\cdot\mathbf{r}) + V_{13}\cos(\mathbf{G}_{31}\cdot\mathbf{r}) + V_{14}\cos(\mathbf{G}_{41}\cdot\mathbf{r}) + V_{23}\cos(\mathbf{G}_{32}\cdot\mathbf{r}) + V_{24}\cos(\mathbf{G}_{42}\cdot\mathbf{r}) + V_{34}\cos(\mathbf{G}_{43}\cdot\mathbf{r})]. \quad (6)$$

The expression results in a DC intensity term and six spatial cosines corresponding to the six interfering-beam pairs. It should be noted that there is a fundamental relationship between the desired reciprocal lattice vectors and the spatial cosine wave vectors. $\mathbf{G}_{21}$, $\mathbf{G}_{31}$, and $\mathbf{G}_{41}$ are equal to **A**, **B**, and **C**, respectively, while $\mathbf{G}_{32}$, $\mathbf{G}_{42}$, and $\mathbf{G}_{43}$ are equal to $(\mathbf{B}-\mathbf{A})$, $(\mathbf{C}-\mathbf{A})$, and $(\mathbf{C}-\mathbf{B})$, respectively.

Here we treat three lattices: simple cubic, face-centered cubic, and body-centered cubic. Using the above methodology, the required recording wave vectors are calculated for the desired translational symmetry given by its primitive lattice vectors. Table 1 summarizes the primitive lattice vectors and the calculated wave vectors. The recording wave vector term k_o is defined as $2\pi/\lambda = |\mathbf{P}|$.

4. Contrast

Proper selection of the recording wave vectors, $\mathbf{k}_i$, has been shown to produce interference patterns with the translational symmetry of all 14 Bravais lattices [43]. The usefulness of an interference pattern for lithography can be improved by systematically selecting the plane wave parameters of the recording beams. This is done most often through nonlinear optimization by maximizing the absolute contrast of

Table 1. Primitive Basis Vectors and their Corresponding Recording Wave Vectors

Lattice	Primitive Lattice Vectors			Wave Vectors			
	a	**b**	**c**	$\mathbf{k}_1$	$\mathbf{k}_2$	$\mathbf{k}_3$	$\mathbf{k}_4$
Cubic	$\frac{\sqrt{3}}{2}\lambda[100]$	$\frac{\sqrt{3}}{2}\lambda[010]$	$\frac{\sqrt{3}}{2}\lambda[001]$	$k_o\frac{1}{\sqrt{3}}[111]$	$k_o\frac{1}{\sqrt{3}}[-111]$	$k_o\frac{1}{\sqrt{3}}[1-11]$	$k_o\frac{1}{\sqrt{3}}[11-1]$
Face-centered cubic	$\frac{3\sqrt{3}}{4}\lambda[110]$	$\frac{3\sqrt{3}}{4}\lambda[011]$	$\frac{3\sqrt{3}}{4}\lambda[101]$	$k_o\frac{1}{3\sqrt{3}}[333]$	$k_o\frac{1}{3\sqrt{3}}[115]$	$k_o\frac{1}{3\sqrt{3}}[511]$	$k_o\frac{1}{3\sqrt{3}}[151]$
Body-centered cubic	$\frac{\sqrt{3}}{4}\lambda[-111]$	$\frac{\sqrt{3}}{4}\lambda[1-11]$	$\frac{\sqrt{3}}{4}\lambda[11-1]$	$k_o\frac{1}{\sqrt{3}}[111]$	$k_o\frac{1}{\sqrt{3}}[1-1-1]$	$k_o\frac{1}{\sqrt{3}}[-11-1]$	$k_o\frac{1}{\sqrt{3}}[-1-11]$

the interference pattern for which the absolute contrast is defined as

$$V_{\text{abs}} = \frac{I_{\max} - I_{\min}}{I_{\max} + I_{\min}}. \tag{7}$$

The nonlinear constraints applied during the optimization determine the locations of symmetry elements and saddle points within the unit cell of the periodic interference pattern. Lithographically speaking, these determine the shape of the intensity contours that will define the final structures. Within four-beam interference, there is one set of nonlinear constraints that has been applied during the optimization process and is referred to in the literature as the *uniform contrast condition* [44,47]. These lithographically useful interference patterns are produced by choosing the plane wave parameters such that all six interference coefficients V_{ij} are equal. Mathematically, the resulting interference patterns have equal contrasts in the three primitive lattice vector directions (**a**, **b**, **c**) from each lattice point. If the assumption about including all six interference coefficients is relaxed, a more fundamental and complete understanding of multibeam interference is possible while still achieving equal contrasts in more than one primitive lattice vector direction. That is, all six interference coefficients do not have to be equal and positive. Avoiding the previously ambiguous terminology of *uniform contrast* [44–46], a more descriptive nomenclature is introduced here, namely, *condition for primitive-lattice-vector-direction equal contrasts*.

In actuality, multiple *conditions for primitive-lattice-vector-direction equal contrasts* exist for MBIL including the four-beam interference case treated here. For three-dimensional periodic interference patterns produced through four-beam interference, there are six spatial cosines as described by Eq. (6). However, only three are required to produce three-dimensional periodicity. Consequently, four *conditions for primitive-lattice-vector-direction equal contrasts* exist. Based on the current research, a symbolic designation $C_n^{(m)}$ is introduced to differentiate between the various *conditions for primitive-lattice-vector-direction equal contrasts*. Quantity n represents the total number of interfering beams and m the number of nonzero interference coefficients (number of interfering beam pairs). Consequently, the resulting nonzero interference coefficients V_{ij} of Eq. (6) are denoted by $V_n^{(m)}$ similarly. In our previously published work for three-beam interference [46], a second *uniform contrast condition* was introduced along with the original *uniform contrast condition*. However, given the new nomenclature and symbolic designation introduced in this work, a more complete description is denoted by $C_3^{(3)}$ and $C_3^{(2)}$ for the first and second *uniform contrast conditions*, respectively, for three-beam interference [46].

Considering our previous work [46] and work that is presented here, it is important to note the relationships between the interference coefficient $V_n^{(m)}$ and the absolute contrast V_{abs}. This suggests that configurations of wave vectors and polarizations can result in interference coefficients that are positive or negative. The physical meaning of this statement is as follows: If a configuration satisfies a *condition for primitive-lattice-vector-direction equal contrasts* and results in a positive interference coefficient, $V_n^{(m)} > 0$, volumes of high intensity surround the lattice points. Similarly, if a configuration satisfies a *condition for primitive-lattice-vector-direction equal contrasts* and results in a negative interference coefficient, $V_n^{(m)} < 0$, volumes of low intensity surround the lattice points. However, regardless of the sign or magnitude of the interference coefficient, $V_n^{(m)}$, determined by the polarization states and amplitudes of the recording beams, the intensity contours will be identical (but differ in intensity value) provided the recording wave vectors remain unchanged. Consequently, another superscript can be added to the given symbolic designation to describe more accurately the interference pattern resulting in ${}^{\pm}C_n^{(m)}$ where $\pm$ denotes either a positive or a negative interference coefficient. This concept of positive and negative interference coefficients enables the pairing of the interference pattern with positive and negative photoresists in a manner analogous to pairing positive and negative photoresist with light- and dark-field masks in conventional lithography. Given a particular lithographic process chemistry, a designer has the ability to choose between these light-field and dark-field interference patterns.

For each lattice, a nonlinear optimization for maximizing absolute contrast is used here to determine the plane wave parameters while satisfying the nonlinear constraints given by each *condition for primitive-lattice-vector-direction equal contrasts*. While subordinate conditions for unity absolute contrast ($V_{\text{abs}} = 1$ with $I_{\min} = 0$) are discussed, these subordinate conditions cannot always be satisfied. However, the nonlinear optimization nevertheless produces solutions that maximize the absolute

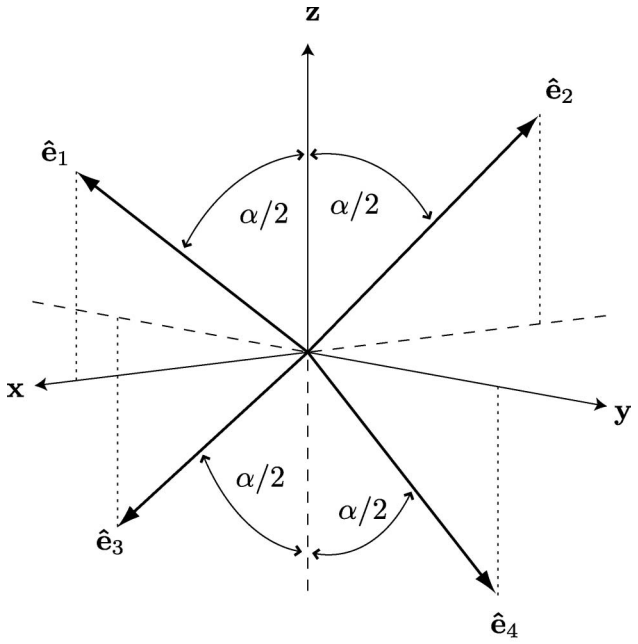

Fig. 1. Orientation of polarizations for the subordinate condition for unity absolute contrast [or any combination of the polarization vectors ($\hat{\mathbf{e}}_i$), where one, multiple, or all are inverted ($-\hat{\mathbf{e}}_i$)] for $^{-}C_4^{(6)}$, where $V_4^{(6)} = -1/3$. $\alpha = \cos^{-1}(-1/3) \approx 109.47°$.

contrast given a particular configuration of recording wave vectors. More detailed information regarding the approach used to determine these optimized parameters is described in the Appendix.

5. Condition for Primitive-Lattice-Vector-Direction Equal Contrasts $C_4^{(6)}$

The previously discussed uniform contrast condition within four-beam interference [44,47] corresponds to a symbolic designation of $C_4^{(6)}$. Each of the six interference coefficients (corresponding to an interfering beam pair) contributes to the modulation of intensity within the interference pattern as

$$V_4^{(6)} = V_{12} = V_{13} = V_{14} = V_{23} = V_{24} = V_{34}[\text{Condition } C_4^{(6)}]. \quad (8)$$

Applying this condition leads to the following set of constraints on the polarizations and amplitudes of the recording beams [44]:

$$e_{12}e_{34} = e_{13}e_{24} = e_{14}e_{23}, \quad (9)$$

$$\frac{E_2}{E_1} = \frac{e_{13}}{e_{23}}, \qquad \frac{E_3}{E_1} = \frac{e_{12}}{e_{23}}, \qquad \frac{E_4}{E_1} = \frac{e_{12}}{e_{24}}. \quad (10)$$

Once these constraints are satisfied, the interference coefficient can be written in terms of the polarization efficiency factors as [44]

$$V_4^{(6)} = \frac{2e_{12}e_{13}e_{23}}{e_{12}^2 + e_{13}^2 + e_{23}^2 + e_{13}^2e_{23}^2/e_{34}^2}. \quad (11)$$

When $C_4^{(6)}$ is satisfied, one set of global intensity extrema (maxima or minima) is located at the lattice points (vertices of the primitive unit cell with the origin at $\mathbf{r} = 0$) and the other set of global intensity extrema (minima or maxima) is located at the face centers of the primitive unit cell ($\mathbf{r} = \mathbf{a}/2 + \mathbf{b}/2$, $\mathbf{r} = \mathbf{a}/2 + \mathbf{c}/2$, $\mathbf{r} = \mathbf{b}/2 + \mathbf{c}/2$). Additional stationary points (saddle points) occur at the body center ($\mathbf{r} = \mathbf{a}/2 + \mathbf{b}/2 + \mathbf{c}/2$) and edge centers ($\mathbf{r} = \mathbf{a}/2$, $\mathbf{r} = \mathbf{b}/2$, $\mathbf{r} = \mathbf{c}/2$) of the primitive unit cell. Given the locations of the intensity extrema, the absolute contrast can be written in terms of the interference coefficient as

$$V_{\text{abs}} = \left|\frac{4}{1/V_4^{(6)} + 2}\right|. \quad (12)$$

A. Subordinate Condition for Unity Absolute Contrast for $^{-}C_4^{(6)}$

Two subordinate conditions also exist for unity absolute contrast ($V_{\text{abs}} = 1$ with $I_{\min} = 0$) for $C_4^{(6)}$. Considering Eq. (12), unity absolute contrast occurs when the interference coefficient $V_4^{(6)}$ equals $-1/6$ or $1/2$. For $V_4^{(6)} = -1/6$, an example of $^{-}C_4^{(6)}$, the additional constraints on the polarizations are

$$e_{ij} = e_{12} = e_{13} = e_{14} = e_{23} = e_{24} = e_{34} = -1/3 \quad (13)$$

Table 2. Optimized Plane Wave Parameters [a] for Lattices Maximizing Absolute Contrast for $^{-}C_4^{(6)}$

Lattice	E_2/E_1	E_3/E_1	E_4/E_1	$\hat{\mathbf{e}}_1$	$\hat{\mathbf{e}}_2$	$\hat{\mathbf{e}}_3$	$\hat{\mathbf{e}}_4$	V	V_{abs}
Simple cubic	1	−1	−1	$\begin{pmatrix}-0.7887\\0.5774\\0.2113\end{pmatrix}$	$\begin{pmatrix}0.2113\\-0.5774\\0.7887\end{pmatrix}$	$\begin{pmatrix}-0.7887\\-0.5774\\0.2113\end{pmatrix}$	$\begin{pmatrix}0.2113\\0.5774\\0.7887\end{pmatrix}$	−1/6	1.0
Face-centered cubic	−4.4930	4.4930	−1.6271	$\begin{pmatrix}0.4083\\-0.8165\\0.4083\end{pmatrix}$	$\begin{pmatrix}-0.7607\\-0.5902\\0.2702\end{pmatrix}$	$\begin{pmatrix}-0.2702\\0.5902\\0.7607\end{pmatrix}$	$\begin{pmatrix}0.6804\\-0.2722\\0.6804\end{pmatrix}$	−0.0575	0.2599
Body-centered cubic	1	−1	−1	$\begin{pmatrix}-0.7887\\0.5774\\0.2113\end{pmatrix}$	$\begin{pmatrix}0.2113\\-0.5774\\0.7887\end{pmatrix}$	$\begin{pmatrix}-0.7887\\-0.5774\\0.2113\end{pmatrix}$	$\begin{pmatrix}0.2113\\0.5774\\0.7887\end{pmatrix}$	−1/6	1.0

[a]Electric field amplitude ratios and polarization vectors with resulting interference coefficient and absolute contrast.

Table 3. Optimized Plane Wave Parameters [a] for Lattices Maximizing Absolute Contrast for ${}^{+}C_4^{(6)}$

Lattice	E_2/E_1	E_3/E_1	E_4/E_1	$\hat{\mathbf{e}}_1$	$\hat{\mathbf{e}}_2$	$\hat{\mathbf{e}}_3$	$\hat{\mathbf{e}}_4$	V	V_{abs}
Simple cubic	0.4472	1	0.4472	$\begin{pmatrix}-0.1310\\-0.6325\\0.7634\end{pmatrix}$	$\begin{pmatrix}0.7071\\0\\0.7071\end{pmatrix}$	$\begin{pmatrix}-0.1310\\0.6325\\0.7634\end{pmatrix}$	$\begin{pmatrix}0.7071\\0\\0.7071\end{pmatrix}$	1/6	1/2
Face-centered cubic	1.2186	1.2186	1.4556	$\begin{pmatrix}0.4083\\-0.8165\\0.4083\end{pmatrix}$	$\begin{pmatrix}0.5455\\-0.8361\\0.0581\end{pmatrix}$	$\begin{pmatrix}0.0581\\-0.8361\\0.5455\end{pmatrix}$	$\begin{pmatrix}0.6804\\-0.2722\\0.6804\end{pmatrix}$	0.3719	0.8531
Body-centered cubic	−0.4472	−0.4472	−1	$\begin{pmatrix}0.1310\\-0.7634\\0.6325\end{pmatrix}$	$\begin{pmatrix}0.7071\\0.7071\\0\end{pmatrix}$	$\begin{pmatrix}0.7071\\0.7071\\0\end{pmatrix}$	$\begin{pmatrix}-0.1310\\0.7634\\0.6325\end{pmatrix}$	1/6	1/2

[a]Electric field amplitude ratios and polarization vectors with resulting interference coefficient and absolute contrast.

(109.47° between polarization vectors) or one of an additional 15 orientations of the polarization vectors that are obtained by inverting $(-\hat{\mathbf{e}}_i)$ any single, any pair, any triplet, or all of the polarization vectors. The orientation of the resulting polarization vectors described in Eq. (13) (which define the vertices of a regular tetrahedron) is illustrated in Fig. 1. For Fig. 1 and subsequent illustrations of the subordinate conditions for unity absolute contrast, the orientations of the polarizations are fixed relative to each other. However, the set of polarization vectors, as a whole, may have any arbitrary rotational orientation relative to the origin. In these illustrations, the specific orientation of the set of polarizations is chosen symmetrically with respect to the Cartesian axes for ease of visualization.

B. Subordinate Condition for Unity Absolute Contrast for ${}^{+}C_4^{(6)}$

For $V_4^{(6)} = 1/2$, an example of ${}^{+}C_4^{(6)}$, the additional constraints on the polarizations are

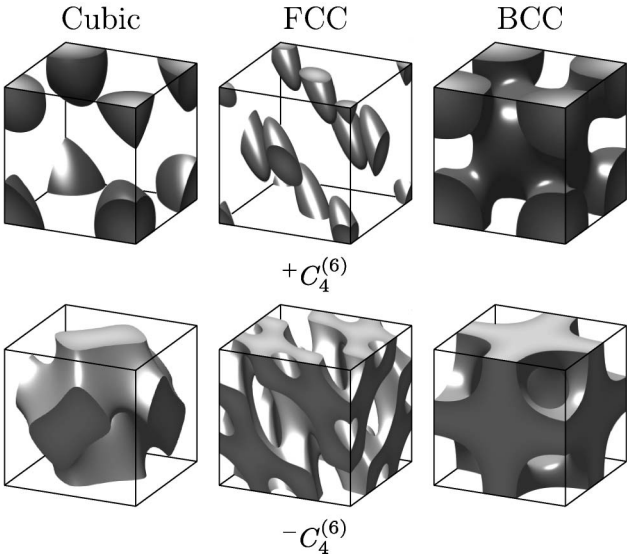

Fig. 2. Intensity contours for interference patterns with body-centered cubic (BCC), face-centered cubic (FCC), and simple cubic periodicity that satisfy the ${}^{+}C_4^{(6)}$ (upper) and ${}^{-}C_4^{(6)}$ (lower) *conditions for primitive-lattice-vector-direction equal contrasts.*

$$e_{ij} = e_{12} = e_{13} = e_{14} = e_{23} = e_{24} = e_{34} = 1 \qquad (14)$$

(parallel polarization vectors) or one of an additional 15 orientations of the polarization vectors that are obtained by inverting $(-\hat{\mathbf{e}}_i)$ any single, any pair, any triplet, or all the polarization vectors. This constraint indicates that the recording wave vectors are coplanar and polarizations are collinear. In this case, the resulting interference pattern will be invariant in at least one direction, i.e., exhibit only two-dimensional periodicity. Thus, optimizing the orientations of polarizations for wave vectors that exhibit three-dimensional periodicity will result in an absolute contrast $V_{\text{abs}} < 1$ while satisfying ${}^{+}C_4^{(6)}$.

A nonlinear optimization to maximize absolute contrast is used to determine the plane wave parameters. Solutions for both ${}^{-}C_4^{(6)}$ and ${}^{+}C_4^{(6)}$ are summarized in Tables 2 and 3, respectively. Intensity contours for each solution are also illustrated in Fig. 2 with volumes of higher intensity being enclosed.

6. Condition for Primitive-Lattice-Vector-Direction Equal Contrasts $C_4^{(5)}$

A second *condition for primitive-lattice-vector-direction equal contrasts* $[C_4^{(5)}]$ occurs when five of the six interference coefficients (corresponding to interfering beam pairs) contribute to the modulation of intensity within the interference pattern as

$$V_4^{(5)} = V_{12} = V_{13} = V_{14} = V_{23} = V_{24},$$
$$V_{34} = 0[\text{Condition } C_4^{(5)}]. \qquad (15)$$

Applying this condition leads to the following set of constraints on the polarizations and amplitudes of the recording beams:

$$e_{13}e_{24} = e_{14}e_{23}, \qquad e_{34} = 0 \qquad (16)$$

(polarization vector $\hat{\mathbf{e}}_3$ orthogonal to $\hat{\mathbf{e}}_4$),

$$\frac{E_2}{E_1} = \frac{e_{13}}{e_{23}}, \qquad \frac{E_3}{E_1} = \frac{e_{12}}{e_{23}}, \qquad \frac{E_4}{E_1} = \frac{e_{12}}{e_{24}}. \qquad (17)$$

Once these constraints are satisfied, the interference coefficient can be written in terms of the polarization efficiency factors as

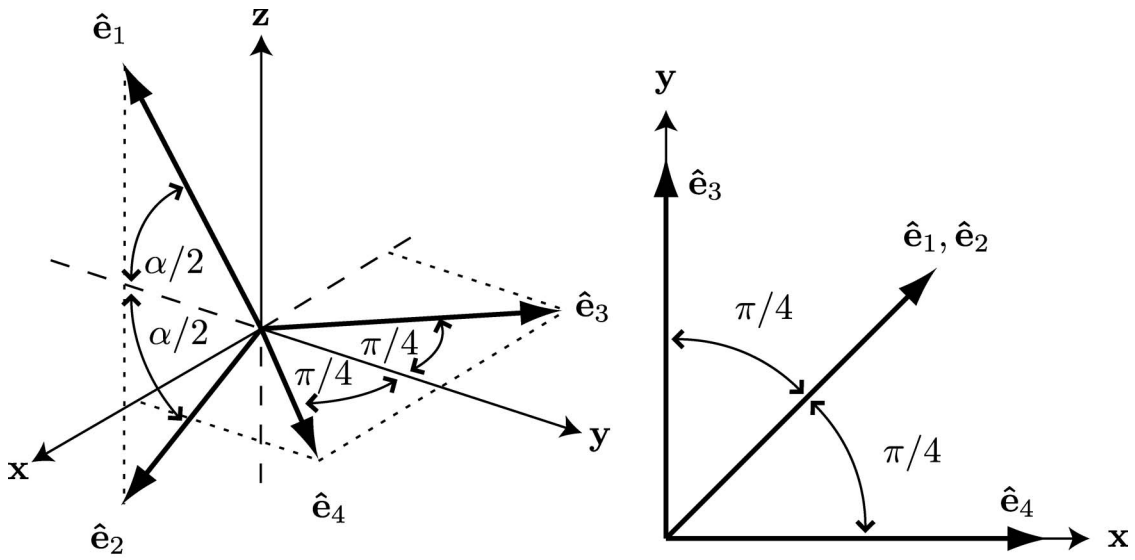

Fig. 3. Orientation of polarizations for the subordinate conditions for unity absolute contrast [or any combination of the polarization vectors ($\hat{\mathbf{e}}_i$), where one, multiple, or all are inverted ($-\hat{\mathbf{e}}_i$)] for (a) $^{+}C_4^{(5)}$, where $V_4^{(5)} = 1/3$ and (b) $^{-}C_4^{(5)}$, where $V_4^{(5)} = -1/3$ and $\alpha = \cos^{-1}(-1/3) \approx 109.47°$.

$$V_4^{(5)} = \frac{2e_{12}e_{13}e_{23}}{e_{12}^2 + e_{13}^2 + e_{23}^2 + e_{12}^2e_{23}^2/e_{24}^2}. \tag{18}$$

When $C_4^{(5)}$ is satisfied, one set of global intensity extrema (maxima or minima) is located at the lattice points (vertices of the primitive unit cell with the origin at $\mathbf{r} = 0$) and the other set of global intensity extrema (minima or maxima) is located at a face center of the primitive unit cell ($\mathbf{r} = \mathbf{b}/2 + \mathbf{c}/2$). Additional stationary points (saddle points) occur at $\mathbf{r} = \mathbf{a}/2 + \mathbf{b}/4 + 3\mathbf{c}/4$, $\mathbf{r} = \mathbf{a}/2 + 3\mathbf{b}/4 + \mathbf{c}/4$, the edge centers ($\mathbf{r} = \mathbf{a}/2$, $\mathbf{r} = \mathbf{b}/2$, $\mathbf{r} = \mathbf{c}/2$), the body center ($\mathbf{r} = \mathbf{a}/2 + \mathbf{b}/2 + \mathbf{c}/2$), and the rest of the face centers ($\mathbf{r} = \mathbf{a}/2 + \mathbf{b}/2$, $\mathbf{r} = \mathbf{a}/2 + \mathbf{c}/2$) of the primitive unit cell. Given the locations of the intensity extrema, the absolute contrast can be written in terms of the interference coefficient as

$$V_{\text{abs}} = \left| \frac{4}{1/V_4^{(5)} + 1} \right|. \tag{19}$$

A. Subordinate Condition for Unity Absolute Contrast for $^{-}C_4^{(5)}$

Two subordinate conditions also exist for unity absolute contrast ($V_{\text{abs}} = 1$ with $I_{\min} = 0$) for $C_4^{(5)}$. Considering Eq. (19), unity absolute contrast occurs when the interference coefficient $V_4^{(5)}$ equals $-1/6$ or $1/3$. For $V_4^{(5)} = -1/6$, an example of $^{-}C_4^{(5)}$, the additional constraints on the polarizations are

$$e_{12} = -1/3, \qquad e_{13} = e_{14} = e_{23} = e_{24} = -1/\sqrt{6} \tag{20}$$

(109.47° or 114.09° between polarization vectors) or one of an additional 15 orientations of the polarization vectors that are obtained by inverting ($-\hat{\mathbf{e}}_i$) any single, any pair, any triplet, or all the polarization vectors. The orientation of the resulting polarization vectors described in Eq. (20) is illustrated in Fig. 3(a).

Table 4. Optimized Plane Wave Parameters [a] for Lattices Maximizing Absolute Contrast for $^{-}C_4^{(5)}$

Lattice	E_2/E_1	E_3/E_1	E_4/E_1	$\hat{\mathbf{e}}_1$	$\hat{\mathbf{e}}_2$	$\hat{\mathbf{e}}_3$	$\hat{\mathbf{e}}_4$	V	V_{abs}
Simple cubic	−1.2214	−1.2214	0.8459	$\begin{pmatrix}-0.7830\\0.1911\\0.5919\end{pmatrix}$	$\begin{pmatrix}-0.2208\\-0.7912\\0.5704\end{pmatrix}$	$\begin{pmatrix}0.1561\\0.7721\\0.6160\end{pmatrix}$	$\begin{pmatrix}0.8148\\-0.4532\\0.3616\end{pmatrix}$	−0.1860	0.9140
Face-centered cubic	−1.8251	−0.53804	1.4018	$\begin{pmatrix}-0.7873\\0.2063\\0.5810\end{pmatrix}$	$\begin{pmatrix}-0.3307\\-0.9105\\0.2482\end{pmatrix}$	$\begin{pmatrix}-0.2718\\0.7163\\0.6427\end{pmatrix}$	$\begin{pmatrix}0.7405\\-0.2711\\0.6150\end{pmatrix}$	−0.1201	0.5461
Body-centered cubic	1.3265	−0.9333	−1.2221	$\begin{pmatrix}-0.7830\\0.5919\\0.1911\end{pmatrix}$	$\begin{pmatrix}0.2208\\-0.5704\\0.7912\end{pmatrix}$	$\begin{pmatrix}-0.8148\\-0.3616\\0.4532\end{pmatrix}$	$\begin{pmatrix}0.1561\\0.6160\\0.7721\end{pmatrix}$	−0.1860	0.9140

[a] Electric field amplitude ratios and polarization vectors with resulting interference coefficient and absolute contrast.

Table 5. Optimized Plane Wave Parameters [a] for Lattices Maximizing Absolute Contrast for ${}^{+}C_4^{(5)}$

Lattice	E_2/E_1	E_3/E_1	E_4/E_1	$\hat{\mathbf{e}}_1$	$\hat{\mathbf{e}}_2$	$\hat{\mathbf{e}}_3$	$\hat{\mathbf{e}}_4$	V	V_{abs}
Simple cubic	1	2	2	$\begin{pmatrix}0.0\\-0.7071\\0.7071\end{pmatrix}$	$\begin{pmatrix}0.0\\-0.7071\\0.7071\end{pmatrix}$	$\begin{pmatrix}-0.7071\\-0.7071\\0.0\end{pmatrix}$	$\begin{pmatrix}0.7071\\-0.7071\\0.0\end{pmatrix}$	1/5	2/3
Face-centered cubic	1	$\sqrt{2}$	$-\sqrt{2}$	$\begin{pmatrix}0.7071\\-0.7071\\0.0\end{pmatrix}$	$\begin{pmatrix}0.7071\\-0.7071\\0.0\end{pmatrix}$	$\begin{pmatrix}0.0969\\-0.9031\\0.4184\end{pmatrix}$	$\begin{pmatrix}-0.9031\\0.0969\\0.4184\end{pmatrix}$	1/3	1.0
Body-centered cubic	1	2	−2	$\begin{pmatrix}0.0\\-0.7071\\0.7071\end{pmatrix}$	$\begin{pmatrix}0.0\\-0.7071\\0.7071\end{pmatrix}$	$\begin{pmatrix}-0.7071\\-0.7071\\0.0\end{pmatrix}$	$\begin{pmatrix}-0.7071\\0.7071\\0.0\end{pmatrix}$	1/5	2/3

[a]Electric field amplitude ratios and polarization vectors with resulting interference coefficient and absolute contrast.

B. Subordinate Condition for Unity Absolute Contrast for ${}^{+}C_4^{(5)}$

For $V_4^{(5)} = 1/3$, an example of ${}^{+}C_4^{(5)}$, the additional constraints on the polarizations are

$$e_{12} = 1, \qquad e_{13} = e_{14} = e_{23} = e_{24} = 1/\sqrt{2} \tag{21}$$

(0° or 45° between polarization vectors) or one of an additional 15 orientations of the polarization vectors that are obtained by inverting $(-\hat{\mathbf{e}}_i)$ any single, any pair, any triplet, or all the polarization vectors. This constraint indicates that all six polarizations are coplanar with $\hat{\mathbf{e}}_3$ and $\hat{\mathbf{e}}_4$ orthogonal and $\hat{\mathbf{e}}_1$ and $\hat{\mathbf{e}}_2$ collinear, bisecting $\hat{\mathbf{e}}_3$ and $\hat{\mathbf{e}}_4$. The orientation of the resulting polarization vectors described in Eq. (21) is illustrated in Fig. 3(b).

A nonlinear optimization to maximize absolute contrast is used to determine the plane wave parameters. Solutions for both ${}^{-}C_4^{(5)}$ and ${}^{+}C_4^{(5)}$ are summarized in Tables 4 and 5, respectively. Intensity contours for each solution are also illustrated in Fig. 4 with volumes of higher intensity being enclosed.

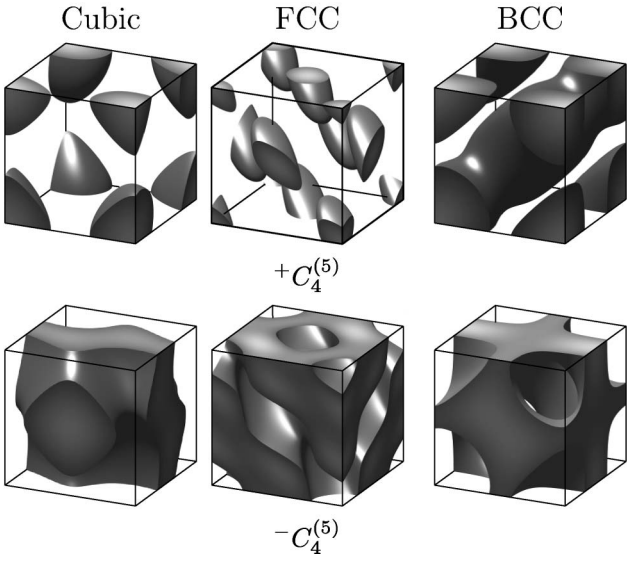

Fig. 4. Intensity contours for interference patterns with body-centered cubic (BCC), face-centered cubic (FCC), and simple cubic periodicity that satisfy the ${}^{+}C_4^{(5)}$ (upper) and ${}^{-}C_4^{(5)}$ (lower) *conditions for primitive-lattice-vector-direction equal contrasts.*

7. Condition for Primitive-Lattice-Vector-Direction Equal Contrasts $C_4^{(4)}$

A third *condition for primitive-lattice-vector-direction equal contrasts* $[C_4^{(4)}]$ occurs when four of the six interference coefficients (corresponding to interfering beam pairs) contribute to the modulation of intensity within the interference pattern as

$$V_4^{(4)} = V_{12} = V_{13} = V_{14} = V_{23},$$
$$V_{24} = V_{34} = 0[\text{Condition } C_4^{(4)}]. \tag{22}$$

Applying this condition leads to the following set of constraints on the polarizations and amplitudes of the recording beams:

$$e_{24} = e_{34} = 0 \tag{23}$$

(polarization vectors are orthogonal),

$$\frac{E_2}{E_1} = \frac{e_{13}}{e_{23}}, \qquad \frac{E_3}{E_1} = \frac{e_{12}}{e_{23}}, \qquad \frac{E_4}{E_1} = \frac{e_{12}e_{13}}{e_{14}e_{23}}. \tag{24}$$

Once these constraints are satisfied, the interference coefficient can be written in terms of the polarization efficiency factors as

$$V_4^{(4)} = \frac{2e_{12}e_{13}e_{23}}{e_{12}^2 + e_{13}^2 + e_{23}^2 + e_{12}^2e_{13}^2/e_{14}^2}. \tag{25}$$

When $C_4^{(4)}$ is satisfied, one set of global intensity extrema (maxima or minima) is located at the lattice points (vertices of the primitive unit cell with the origin at $\mathbf{r} = 0$) and the other set of global intensity extrema (minima or maxima) is located at $\mathbf{r} = \mathbf{a}/3 + 2\mathbf{b}/3 + \mathbf{c}/2$ and $\mathbf{r} = 2\mathbf{a}/3 + \mathbf{b}/3 + \mathbf{c}/2$. Additional stationary points (saddle points) occur at the edge centers ($\mathbf{r} = \mathbf{a}/2$, $\mathbf{r} = \mathbf{b}/2$, $\mathbf{r} = \mathbf{c}/2$), body center ($\mathbf{r} = \mathbf{a}/2 + \mathbf{b}/2 + \mathbf{c}/2$), and face centers ($\mathbf{r} = \mathbf{a}/2 + \mathbf{b}/2$, $\mathbf{r} = \mathbf{a}/2 + \mathbf{c}/2$, $\mathbf{r} = \mathbf{b}/2 + \mathbf{c}/2$) of the primitive unit cell, and also at $\mathbf{r} = \mathbf{a}/3 + 2\mathbf{b}/3$, and $\mathbf{r} = 2\mathbf{a}/3 + \mathbf{b}/3$. Given the locations of the intensity extrema, the absolute contrast is written in terms of the interference coefficient as

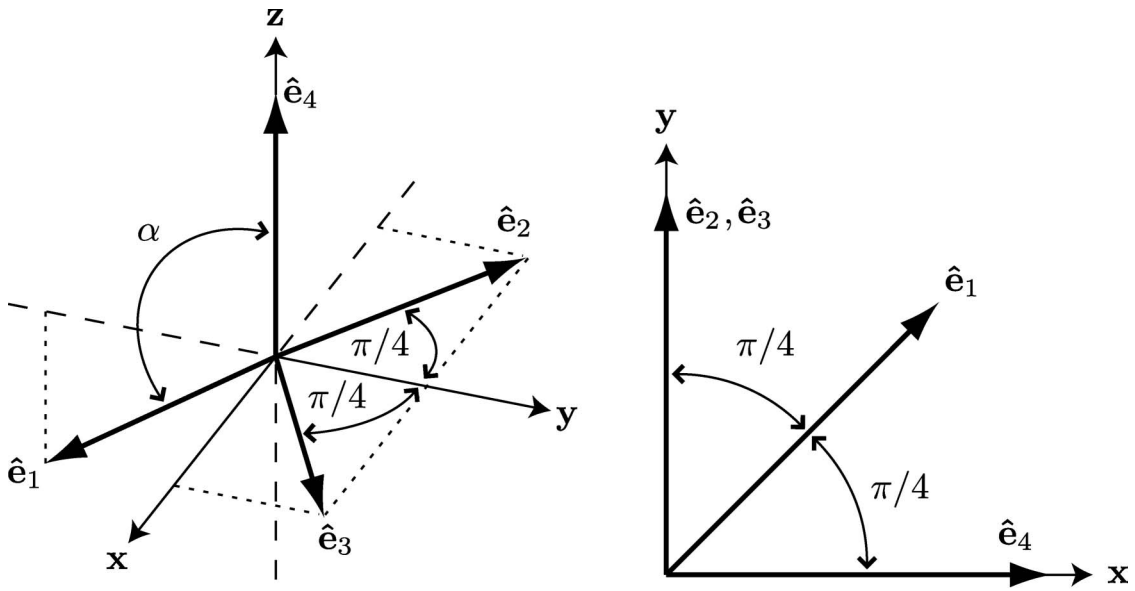

(a) $^{-}C_4^{(4)}$ (b) $^{+}C_4^{(4)}$

Fig. 5. Orientation of polarizations for the subordinate conditions for unity absolute contrast [or any combination of the polarization vectors ($\hat{\mathbf{e}}_i$), where one, multiple, or all are inverted ($-\hat{\mathbf{e}}_i$)] for (a) $^{+}C_4^{(4)}$, where $V_4^{(4)} = 2/5$ and (b) $^{-}C_4^{(4)}$ where $V_4^{(4)} = -1/4$ and $\alpha = \cos^{-1}(1/\sqrt{3}) \approx 125.26°$.

$$V_{\text{abs}} = \left| \frac{13}{4/V_4^{(4)} + 3} \right|. \tag{26}$$

A. Subordinate Condition for Unity Absolute Contrast for $^{-}C_4^{(4)}$

Two subordinate conditions also exist for unity absolute contrast ($V_{\text{abs}} = 1$ with $I_{\min} = 0$) for $C_4^{(4)}$. Considering Eq. (26), unity absolute contrast occurs when the interference coefficient $V_4^{(4)}$ equals $-1/4$ or $2/5$. For $V_4^{(4)} = -1/4$, an example of $^{-}C_4^{(4)}$, the additional constraints on the polarizations are

$$e_{12} = e_{13} = -1/\sqrt{6}, \qquad e_{14} = -1/\sqrt{3}, \qquad e_{23} = -1/2 \tag{27}$$

(114.09°, 125.26°, or 120° between polarization vectors) or one of an additional 15 orientations of the polarization vectors that are obtained by inverting ($-\hat{\mathbf{e}}_i$) any single, any pair, any triplet, or all the polarization vectors. The orientation of the resulting polarization vectors described in Eq. (27) is illustrated in Fig. 5(a).

B. Subordinate Condition for Unity Absolute Contrast for $^{+}C_4^{(4)}$

For $V_4^{(4)} = 2/5$, an example of $^{+}C_4^{(4)}$, the additional constraints on the polarizations are

$$e_{12} = e_{13} = e_{14} = 1/\sqrt{2}, \qquad e_{23} = 1 \tag{28}$$

(45° or 0° between polarization vectors) or one of an additional 15 orientations of the polarization vectors that are obtained by inverting ($-\hat{\mathbf{e}}_i$) any single, any pair, any triplet, or all the polarization vectors. This constraint indicates that all six polarizations are coplanar with $\hat{\mathbf{e}}_4$ orthogonal to $\hat{\mathbf{e}}_2$ and $\hat{\mathbf{e}}_3$ (which are collinear) and $\hat{\mathbf{e}}_1$ bisecting $\hat{\mathbf{e}}_2$ and $\hat{\mathbf{e}}_4$. The orientation

Table 6. Optimized Plane Wave Parameters [a] for Lattices Maximizing Absolute Contrast for $^{-}C_4^{(4)}$

Lattice	E_2/E_1	E_3/E_1	E_4/E_1	$\hat{\mathbf{e}}_1$	$\hat{\mathbf{e}}_2$	$\hat{\mathbf{e}}_3$	$\hat{\mathbf{e}}_4$	V	V_{abs}
Simple cubic	−0.78901	0.7769	−0.5049	$\begin{pmatrix} 0.6395 \\ -0.7594 \\ 0.1199 \end{pmatrix}$	$\begin{pmatrix} -0.4298 \\ -0.8161 \\ 0.3863 \end{pmatrix}$	$\begin{pmatrix} -0.6613 \\ 0.0841 \\ 0.7454 \end{pmatrix}$	$\begin{pmatrix} 0.7417 \\ -0.0752 \\ 0.6665 \end{pmatrix}$	−0.2488	0.9942
Face-centered cubic	−0.8742	0.8915	−0.3104	$\begin{pmatrix} -0.1980 \\ -0.5870 \\ 0.7850 \end{pmatrix}$	$\begin{pmatrix} -0.9810 \\ 0.0610 \\ 0.1840 \end{pmatrix}$	$\begin{pmatrix} -0.2392 \\ 0.9353 \\ 0.2608 \end{pmatrix}$	$\begin{pmatrix} 0.1661 \\ -0.2252 \\ 0.9601 \end{pmatrix}$	−0.1994	0.7620
Body-centered cubic	0.7769	−0.78901	−0.5049	$\begin{pmatrix} -0.7594 \\ 0.6395 \\ 0.1199 \end{pmatrix}$	$\begin{pmatrix} 0.0841 \\ -0.6613 \\ 0.7454 \end{pmatrix}$	$\begin{pmatrix} -0.8161 \\ -0.4298 \\ 0.3863 \end{pmatrix}$	$\begin{pmatrix} -0.0752 \\ 0.7417 \\ 0.6665 \end{pmatrix}$	−0.2488	0.9942

[a] Electric field amplitude ratios and polarization vectors with resulting interference coefficient and absolute contrast.

Table 7. Optimized Plane Wave Parameters [a] for Lattices Maximizing Absolute Contrast for ${}^{+}C_4^{(4)}$

Lattice	E_2/E_1	E_3/E_1	E_4/E_1	$\hat{\mathbf{e}}_1$	$\hat{\mathbf{e}}_2$	$\hat{\mathbf{e}}_3$	$\hat{\mathbf{e}}_4$	V	V_{abs}
Simple cubic	−0.5956	0.4575	0.4782	$\begin{pmatrix}-0.7193\\0.0251\\0.6942\end{pmatrix}$	$\begin{pmatrix}0.7588\\0.6405\\0.1183\end{pmatrix}$	$\begin{pmatrix}-0.7473\\-0.6585\\0.0888\end{pmatrix}$	$\begin{pmatrix}-0.6509\\0.7524\\0.1015\end{pmatrix}$	0.2974	0.7903
Face-centered cubic	−0.7226	−0.6966	0.6943	$\begin{pmatrix}-0.7201\\0.6934\\0.0268\end{pmatrix}$	$\begin{pmatrix}0.0071\\-0.9808\\0.1947\end{pmatrix}$	$\begin{pmatrix}0.1083\\-0.9195\\0.3779\end{pmatrix}$	$\begin{pmatrix}-0.8840\\0.0849\\0.4598\end{pmatrix}$	0.3948	0.9899
Body-centered cubic	0.4575	−0.5956	0.4782	$\begin{pmatrix}0.0251\\-0.7193\\0.6942\end{pmatrix}$	$\begin{pmatrix}-0.6585\\-0.7473\\0.0888\end{pmatrix}$	$\begin{pmatrix}0.6405\\0.7588\\0.1183\end{pmatrix}$	$\begin{pmatrix}0.7524\\-0.6509\\0.1015\end{pmatrix}$	0.2974	0.7903

[a]Electric field amplitude ratios and polarization vectors with resulting interference coefficient and absolute contrast.

of the resulting polarization vectors described in Eq. (28) is illustrated in Fig. 5(b).

A nonlinear optimization to maximize absolute contrast is used to determine the plane wave parameters. Solutions for both ${}^{-}C_4^{(4)}$ and ${}^{+}C_4^{(4)}$ are summarized in Tables 6 and 7, respectively. Intensity contours for each solution are also illustrated in Fig. 6 with volumes of higher intensity being enclosed.

8. Condition for Primitive-Lattice-Vector-Direction Equal Contrasts $C_4^{(3)}$

The fourth, and final, *condition for primitive-lattice-vector-direction equal contrasts* [$C_4^{(3)}$] occurs when three of the six interference coefficients (corresponding to interfering beam pairs) contribute to the modulation of intensity within the interference pattern as

$$V_4^{(3)} = V_{12} = V_{13} = V_{14},$$
$$V_{23} = V_{24} = V_{34} = 0 [\text{Condition } C_4^{(3)}]. \quad (29)$$

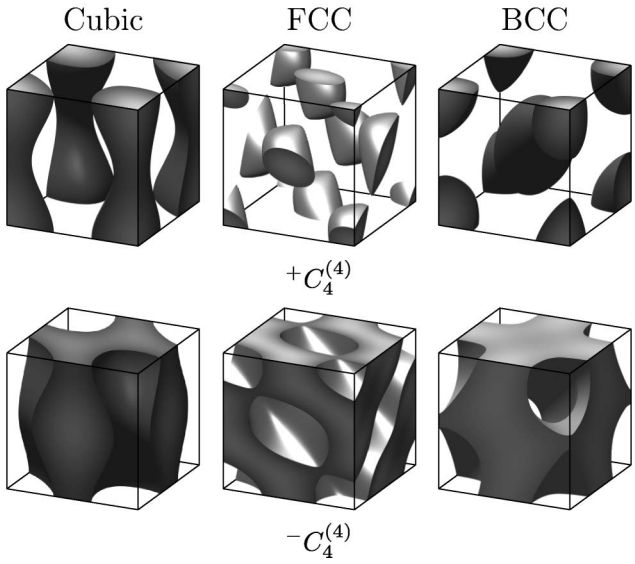

Fig. 6. Intensity contours for interference patterns with body-centered cubic (BCC), face-centered cubic (FCC), and simple cubic periodicity that satisfy the ${}^{+}C_4^{(4)}$ (upper) and ${}^{-}C_4^{(4)}$ (lower) *conditions for primitive-lattice-vector-direction equal contrasts.*

Applying this condition leads to the following set of constraints on the polarizations and amplitudes of the recording beams:

$$e_{23} = e_{24} = e_{34} = 0 \quad (30)$$

(polarization vectors are orthogonal),

$$\frac{E_3}{E_2} = \frac{e_{12}}{e_{13}}, \qquad \frac{E_4}{E_2} = \frac{e_{12}}{e_{14}}. \quad (31)$$

Once these constraints are satisfied, the interference coefficient can be written in terms of the polarization efficiency factors as

$$V_4^{(3)} = \frac{2E_1E_2e_{12}}{E_1^2 + E_2^2(1 + e_{12}^2/e_{13}^2 + e_{12}^2/e_{14}^2)}. \quad (32)$$

When $C_4^{(3)}$ is satisfied, one set of global intensity extrema (maxima or minima) is located at the lattice points (vertices of the primitive unit cell with the origin at $\mathbf{r} = 0$) and the other set of global intensity extrema (minima or maxima) is located at the body center of the primitive unit cell ($\mathbf{r} = \mathbf{a}/2 + \mathbf{b}/2 + \mathbf{c}/2$). Additional stationary points (saddle points) occur at the edge centers ($\mathbf{r} = \mathbf{a}/2$, $\mathbf{r} = \mathbf{b}/2$, $\mathbf{r} = \mathbf{c}/2$) and the face centers ($\mathbf{r} = \mathbf{a}/2 + \mathbf{b}/2$, $\mathbf{r} = \mathbf{a}/2 + \mathbf{c}/2$, $\mathbf{r} = \mathbf{b}/2 + \mathbf{c}/2$) of the primitive unit cell. Given the locations of the intensity extrema, the absolute contrast can be written in terms of the interference coefficient as

$$V_{\text{abs}} = |3V_4^{(3)}|. \quad (33)$$

Given a configuration of polarizations that satisfy Eqs. (30) and (31), the absolute contrast [or interference coefficient in Eq. (32)] can be maximized by setting the electric field ratio E_2/E_1 equal to

$$\frac{E_2}{E_1} = \frac{1}{\sqrt{1 + e_{12}^2/e_{13}^2 + e_{12}^2/e_{14}^2}}. \quad (34)$$

The interference coefficient can then be rewritten solely in terms of polarization as

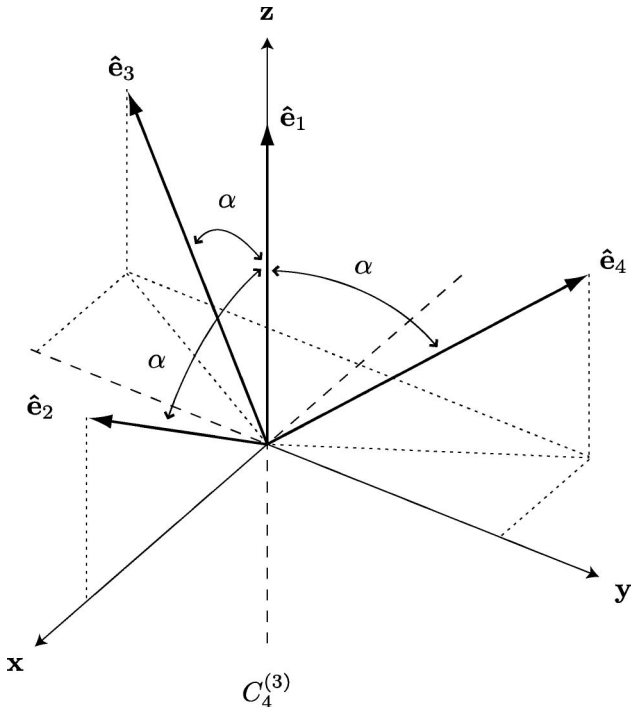

Fig. 7. Orientation of polarizations for the subordinate conditions for unity absolute contrast [or any combination of the polarization vectors ($\hat{\mathbf{e}}_i$), where one, multiple, or all are inverted ($-\hat{\mathbf{e}}_i$)] for $C_4^{(3)}$, where $V_4^{(3)} = \pm 1/3$ and $\alpha = \cos^{-1}(\sqrt{3}/3) \approx 54.74°$.

$$V_4^{(3)} = \frac{e_{12}e_{13}e_{14}}{\sqrt{e_{13}^2e_{14}^2 + e_{12}^2e_{14}^2 + e_{12}^2e_{13}^2}}. \tag{35}$$

Generally speaking, there is no difference in interference patterns satisfying ${}^{-}C_4^{(3)}$ and ${}^{+}C_4^{(3)}$ in that the contours around intensity maxima and minima are identical (differing only in intensity value). This particular *condition for primitive-lattice-vector-direction equal contrasts* in three dimensions is similar to the *condition for primitive-lattice-vector-direction equal contrasts* in two dimensions designated as $C_3^{(2)}$ (previously referred to as the *second uniform contrast condition* in two dimensions) in this regard [46]. Given a bias intensity value of I_b (where $I_{\min} \le I_b \le I_{\max}$), these two identical surfaces are described as

$$I_{\max} - I_b = I(\mathbf{r}),$$
$$I_{\min} + I_b = I(\mathbf{r} + \mathbf{a}/2 + \mathbf{b}/2 + \mathbf{c}/2). \tag{36}$$

While the interference coefficient $V_4^{(3)}$ of a specific solution that satisfies $C_4^{(3)}$ will be positive or negative, this metric simply describes whether interference maxima or minima are located at lattice points ($\mathbf{r} = 0$ and all equivalent points in the periodic interference pattern). Two interference patterns with coefficients of $V_4^{(3)}$ and $-V_4^{(3)}$ are identical when either is translated by $\mathbf{a}/2 + \mathbf{b}/2 + \mathbf{c}/2$.

A. Subordinate Condition for Unity Absolute Contrast for $C_4^{(3)}$

One subordinate condition exists for unity absolute contrast ($V_{\text{abs}} = 1$ with $I_{\min} = 0$) for $C_4^{(3)}$. Considering Eq. (33), unity absolute contrast occurs when the interference coefficient $V_4^{(3)}$ equals $-1/3$ or $1/3$. The additional constraints on the polarizations are

$$e_{12} = e_{13} = e_{14} = 1/\sqrt{3} \tag{37}$$

(54.74° between polarization vectors) or one of an additional 15 orientations of the polarization vectors that are obtained by inverting ($-\hat{\mathbf{e}}_i$) any single, any pair, any triplet, or all the polarization vectors. The orientation of the resulting polarization vectors described in Eq. (37) is illustrated in Fig. 7.

A nonlinear optimization to maximize absolute contrast is used to determine the plane wave parameters. Solutions for $C_4^{(3)}$ are summarized in Table 8. Intensity contours for each solution are also illustrated in Fig. 8 with volumes of higher intensity being enclosed.

9. Summary and Discussion

Optimized solutions for three different lattices with all four different *conditions for primitive-lattice-vector-direction equal contrasts* in three dimensions exhibiting the maximum possible absolute contrast have been given in Tables 3 through 8. These tables provide guidelines for determining lithographic process parameters and enable choosing between processes based on positive-tone or negative-tone photoresists. The lithographic process

Table 8. Optimized Plane Wave Parameters [a] for Lattices Maximizing Absolute Contrast for ${}^{+}C_4^{(3)}$

Lattice	E_2/E_1	E_3/E_1	E_4/E_1	$\hat{\mathbf{e}}_1$	$\hat{\mathbf{e}}_2$	$\hat{\mathbf{e}}_3$	$\hat{\mathbf{e}}_4$	V	V_{abs}
Simple cubic	2/3	−2/3	1/3	$\begin{pmatrix}0.5826\\-0.7867\\0.2041\end{pmatrix}$	$\begin{pmatrix}-0.5000\\-0.8090\\0.3090\end{pmatrix}$	$\begin{pmatrix}-0.3090\\0.5000\\0.8090\end{pmatrix}$	$\begin{pmatrix}0.8090\\-0.3090\\0.5000\end{pmatrix}$	$\sqrt{6}/9$	$\sqrt{6}/3$
Face-centered cubic	2/3	1/3	−2/3	$\begin{pmatrix}-0.7144\\0.6995\\0.0149\end{pmatrix}$	$\begin{pmatrix}-0.9045\\-0.3455\\0.2500\end{pmatrix}$	$\begin{pmatrix}-0.2500\\0.9045\\0.3455\end{pmatrix}$	$\begin{pmatrix}0.3455\\-0.2500\\0.9045\end{pmatrix}$	$\sqrt{6}/9$	$\sqrt{6}/3$
Body-centered cubic	1/3	2/3	2/3	$\begin{pmatrix}-0.2041\\-0.5826\\0.7867\end{pmatrix}$	$\begin{pmatrix}-0.5000\\-0.8090\\0.3090\end{pmatrix}$	$\begin{pmatrix}-0.3090\\0.5000\\0.8090\end{pmatrix}$	$\begin{pmatrix}0.8090\\-0.3090\\0.5000\end{pmatrix}$	$\sqrt{6}/9$	$\sqrt{6}/3$

[a] Electric field amplitude ratios and polarization vectors with resulting interference coefficient and absolute contrast.

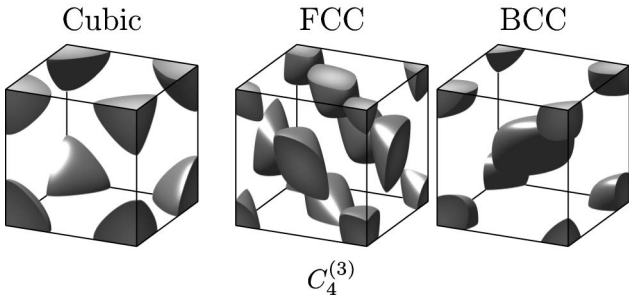

Fig. 8. Intensity contours for interference patterns with body-centered cubic (BCC), face-centered cubic (FCC), and simple cubic periodicity that satisfy the $C_4^{(3)}$ *condition for primitive-lattice-vector-direction equal contrasts*.

will be easier to implement and will provide greater processing latitude when an interference pattern with the largest absolute contrast is used.

From the quantitative descriptions of the *conditions for primitive-lattice-vector-direction equal contrasts* and the illustrations of the intensity contours for the three lattices, a more qualitative description of the resultant interference patterns can be given. For the $C_4^{(6)}$ and $C_4^{(3)}$, there is equal contrast in each of the primitive lattice directions (**a**, **b**, and **c**) from each lattice point. For $C_4^{(5)}$, there is equal contrast in two of the primitive lattice directions (**a** and **c**) from each lattice point. For $C_4^{(4)}$, there is equal contrast in two of the primitive lattice directions (**a** and **b**) from each lattice point. For the three lattices treated, there are significant differences in the absolute contrast of the optimized solutions between each *condition for primitive-lattice-vector-direction equal contrasts* and between the distinct ${}^{+}C_n^{(m)}$ and ${}^{-}C_n^{(m)}$ solutions. For the simple cubic lattice, the absolute contrast ranges from 0.5 when satisfying ${}^{+}C_4^{(6)}$ to unity absolute contrast when satisfying ${}^{-}C_4^{(6)}$. For the face-centered cubic lattice, the absolute contrast ranges from 0.2599 when satisfying ${}^{-}C_4^{(6)}$ to unity absolute contrast when satisfying ${}^{+}C_4^{(5)}$. For the body-centered cubic lattice, the absolute contrast ranges from 0.5 when satisfying ${}^{+}C_4^{(6)}$ to unity absolute contrast when satisfying ${}^{-}C_4^{(6)}$. We have presented four different conditions in the case of four-beam interference that will result in lithographically useful interference patterns suitable for lithographic processing. Four-beam interference also serves as a basis for determining and describing these interference patterns in terms of the crystallographic space groups that determine the symmetry of the patterns.

Appendix: Optimization Approaches

To maximize the absolute contrast, an objective function must be maximized (or minimized) under constraints given by the physical problem and by each *condition for primitive-lattice-vector-direction equal contrasts*. In the most general of terms, this problem will have 12 variables and either 10 or 11 constraint equations (depending on the *condition for primitive-lattice-vector-direction equal contrasts*). The 12 variables are the 12 Cartesian coordinates that describe each of the four polarization vectors as

$$\hat{\mathbf{e}}_i = (e_{i,x}, e_{i,y}, e_{i,z}). \tag{A1}$$

Each polarization vector must be normalized

$$|\hat{\mathbf{e}}_i| = \sqrt{e_{i,x}^2 + e_{i,y}^2 + e_{i,z}^2} = 1 \tag{A2}$$

and orthogonal to its corresponding wave vector

$$\hat{\mathbf{e}}_i \cdot \mathbf{k}_i = e_{i,x}k_{i,x} + e_{i,y}k_{i,y} + e_{i,z}k_{i,z} = 0, \tag{A3}$$

where the wave vector is

$$\mathbf{k}_i = (k_{i,x}, k_{i,y}, k_{i,z}). \tag{A4}$$

Equations (A2) and (A3) constitute eight of the constraint equations (two for each recording wave vector). The final two or three constraint equations are determined by the *condition for primitive-lattice-vector-direction equal contrasts* in Eq. (9) for $C_4^{(6)}$, in Eq. (16) for $C_4^{(5)}$, in Eq. (23) for $C_4^{(4)}$, and in Eq. (30) for $C_4^{(3)}$. The objective function, absolute contrast, is calculated in terms of these 12 variables and maximized under the 10 or 11 constraint equations.

A commonly used strategy for solving constrained optimization problems is the method of Lagrange multipliers. Given the function to be minimized or maximized,

$$f(x_1, \ldots, x_n), \tag{A5}$$

subject to the constraint equations

$$g_1(x_1, \ldots, x_n) = c_1, \ldots, g_m(x_1, \ldots, x_n) = c_m, \tag{A6}$$

the Lagrangian function is written as

$$\begin{aligned}\Lambda(x_1, \ldots, x_n, \lambda_1, \ldots, \lambda_m) = f(x_1, \ldots, x_n) \\ + \lambda_1(g_1(x_1, \ldots, x_n) - c_1) \\ + \ldots + \lambda_m(g_m(x_1, \ldots, x_n) - c_m)\end{aligned} \tag{A7}$$

with the introduction of m Lagrange multipliers (λ_i). A subset of the stationary points of this unconstrained function, given by

$$\nabla\Lambda = 0, \tag{A8}$$

is the solution to the constrained optimization problem. As described above, the constrained optimization problem of 12 variables and 10 or 11 constraint equations yields a Lagrangian function of 22 or 23 variables (constituting 10 or 11 Lagrange multipliers).

For this work, however, we utilized a different approach that incorporates only four variables and two or three constraint equations. The four variables are the counterclockwise angular rotations (when looking antiparallel to the wave vector $\mathbf{k}_i$), ψ_i, of the vector

$$\hat{\mathbf{e}}_{i,0} = \hat{\mathbf{z}} \times \mathbf{k}_i \tag{A9}$$

about $\mathbf{k}_i$, which corresponds to a polarization vector $\hat{\mathbf{e}}_i$, for wave vector $\mathbf{k}_i$. This is accomplished by applying five rotational transformations to $\hat{\mathbf{e}}_{i,0}$. Given the rotational matrices for the counterclockwise angular rotation (when looking toward the origin) of the x, y, and z axes as $\mathbf{R}_x(\alpha)$, $\mathbf{R}_y(\beta)$, and $\mathbf{R}_z(\gamma)$, respectively, ψ_i describes the polarization vector $\hat{\mathbf{e}}_i$ as

$$\hat{\mathbf{e}}_i = \mathbf{R}_z(-\phi)\mathbf{R}_y(-\theta)\mathbf{R}_z(-\psi)\mathbf{R}_y(\theta)\mathbf{R}_z(\phi)\hat{\mathbf{e}}_{i,0}, \tag{A10}$$

where θ and ϕ are the spherical coordinates of $\mathbf{k}_i$. By definition, $\hat{\mathbf{e}}_{i,0}$ and $\hat{\mathbf{e}}_i$ satisfy the orthogonality and normalized conditions, eliminating the need to incorporate the eight constraint equations given by Eqs. (A2) and (A3). The objective function, absolute contrast, is then calculated in terms of these four variables and maximized under the two or three constraint equations given by each *condition for primitive-lattice-vector-direction equal contrasts*. This results in a Lagrangian function of only six or seven variables (constituting two or three Lagrange multipliers). This approach resulted in a quicker and more stable implementation of the nonlinear optimization.

This research was supported in part by the National Science Foundation (NSF) under grant ECCS-0925119. .

References

1. J. D. Joannopoulos, S. G. Johnson, J. N. Winn, and R. D. Meade, *Photonic Crystals: Molding the Flow of Light* (Princeton U. Press, 2008).
2. A. Di Falco, C. Conti, and G. Assanto, "Three-dimensional superprism effect in photonic-crystal slabs," J. Lightwave Technol. **22**, 1748–1753 (2004).
3. H. Kosaka, T. Kawashima, A. Tomita, M. Notomi, T. Tamamura, T. Sato, and S. Kawakami, "Superprism phenomena in photonic crystals: toward microscale lightwave circuits," J. Lightwave Technol. **17**, 2032–2038 (1999).
4. T. Matsumoto and T. Baba, "Photonic crystal k-vector superprism," J. Lightwave Technol. **22**, 917–922 (2004).
5. A. Locatelli, M. Conforti, D. Modotto, and C. De Angelis, "Discrete negative refraction in photonic crystal waveguide arrays," Opt. Lett. **31**, 1343–1345 (2006).
6. M. Qiu, L. Thylen, M. Swillo, and B. Jaskorzynska, "Wave propagation through a photonic crystal in a negative phase refractive-index region," IEEE J. Sel. Top. Quantum Electron. **9**, 106–110 (2003).
7. J. Witzens, T. Baehr-Jones, and A. Scherer, "Hybrid superprism with low insertion losses and suppressed cross-talk," Phys. Rev. E **71**, 026604 (2005).
8. T. Matsumoto, S. Fujita, and T. Baba, "Wavelength demultiplexer consisting of photonic crystal superprism and superlens," Opt. Express **13**, 10768–10783 (2005).
9. B. Momeni, J. Huang, M. Soltani, M. Askari, S. Mohammadi, M. Rakhshandehroo, and A. Adibi, "Compact wavelength demultiplexing using focusing negative index photonic crystal superprisms," Opt. Express **14**, 2413–2422 (2006).
10. A. Adibi, Y. Xu, R. K. Lee, A. Yariv, and A. Scherer, "Properties of the slab modes in photonic crystal optical waveguides," J. Lightwave Technol. **18**, 1554–1564 (2000).
11. A. Jafarpour, E. Chow, C. M. Reinke, J. Huang, A. Adibi, A. Grot, L. W. Mirkarimi, G. Girolami, R. K. Lee, and Y. Xu, "Large-bandwidth ultra-low-loss guiding in bi-periodic photonic crystal waveguides," Appl. Phys. B **79**, 409–414 (2004).
12. M. M. Beaky, J. B. Burk, H. O. Everitt, M. A. Haider, and S. Venakides, "Two-dimensional photonic crystal Fabry-Perot resonators with lossy dielectrics," IEEE Trans. Microwave Theory Tech. **47**, 2085–2091 (1999).
13. P. Kramper, A. Birner, M. Agio, C. M. Soukoulis, F. Muller, U. Gosele, J. Mlynek, and V. Sandoghdar, "Direct spectroscopy of a deep two-dimensional photonic crystal microresonator," Phys. Rev. B **64**, 233102-1–233102-4 (2001).
14. P. Kramper, M. Kafesaki, C. M. Soukoulis, A. Birner, F. Muller, U. Gosele, R. B. Wehrspohn, J. Mlynek, and V. Sandoghdar, "Near-field visualization of light confinement in a photonic crystal microresonator," Opt. Lett. **29**, 174–176 (2004).
15. T. Kim and C. Seo, "A novel photonic bandgap structure for low-pass filter of wide stopband," IEEE Microwave Guid. Wave Lett. **10**, 13–15 (2000).
16. R. C. Rumpf, A. Mehta, P. Srinivasan, and E. G. Johnson, "Design and optimization of space-variant photonic crystal filters," Appl. Opt. **46**, 5755–5761 (2007).
17. A. Mehta, R. Rumpf, Z. Roth, and E. G. Johnson, "Simplified fabrication process of 3-D photonic crystal optical transmission filter," Proc. SPIE **6462**, 64621D (2007).
18. B. Z. Steinberg, A. Boag, and R. Lisitsin, "Sensitivity analysis of narrowband photonic crystal filters and waveguides to structure variations and inaccuracy," J. Opt. Soc. Am. A **20**, 138–146 (2003).
19. T. Kamalakis and T. Sphicopoulos, "Numerical study of the implications of size nonuniformities in the performance of photonic crystal couplers using coupled mode theory," IEEE J. Quantum Electron. **41**, 863–871 (2005).
20. C.-Y. Liu and L.-W. Chen, "Tunable photonic crystal waveguide coupler with nematic liquid crystals," IEEE Photon. Technol. Lett. **16**, 1849–1851 (2004).
21. A. Mekis and J. D. Joannopoulos, "Tapered couplers for efficient interfacing between dielectric and photonic crystal waveguides," J. Lightwave Technol. **19**, 861–865 (2001).
22. Y. Tanaka, H. Nakamura, Y. Sugimoto, N. Ikeda, K. Asakawa, and K. Inoue, "Coupling properties in a 2-D photonic crystal slab directional coupler with a triangular lattice of air holes," IEEE J. Quantum Electron. **41**, 76–84 (2005).
23. M. Thorhauge, L. H. Frandsen, and P. I. Borel, "Efficient photonic crystal directional couplers," Opt. Lett. **28**, 1525–1527 (2003).
24. B. Momeni and A. Adibi, "Demultiplexers harness photonic-crystal dispersion properties," Laser Focus World **42**, 125–128 (2006).
25. C. Caloz, A. K. Skrivervik, and F. E. Gardiol, "An efficient method to determine Green's functions of a two-dimensional photonic crystal excited by a line source—the phased-array method," IEEE Trans. Microwave Theory Tech. **50**, 1380–1391 (2002).

26. T. Tanabe, M. Notomi, S. Mitsugi, A. Shinya, and E. Kuramochi, "All-optical switches on a silicon chip realized using photonic crystal nanocavities," Appl. Phys. Lett. **87**, 151112 (2005).
27. S. Chakravarty, J. Topol'ancik, P. Bhattacharya, S. Chakrabarti, Y. Kang, and M. E. Meyerhoff, "Ion detection with photonic crystal microcavities," Opt. Lett. **30**, 2578–2580 (2005).
28. J. Serbin, A. Ovsianikov, and B. Chichkov, "Fabrication of woodpile structures by two-photon polymerization and investigation of their optical properties," Opt. Express **12**, 5221–5228 (2004).
29. S. Kawata, H.-B. Sun, T. Tanaka, and K. Takada, "Finer features for functional microdevices," Nature **412**, 697–698 (2001).
30. S. Cabrini, L. Businaro, M. Prasciolu, A. Carpentiro, D. Gerace, M. Galli, L. C. Andreani, F. Riboli, L. Pavesi, and E. Di Fabrizio, "Focused ion beam fabrication of one-dimensional photonic crystals on Si_3N_4/SiO_2 channel waveguides," J. Opt. A: Pure Appl. Opt. **8**, 550–553 (2006).
31. A. P. Hynninen, J. H. J. Thijssen, E. C. M. Vermolen, M. Dijkstra, and A. Van Blaaderen, "Self-assembly route for photonic crystals with a bandgap in the visible region," Nat. Mater. **6**, 202–205 (2007).
32. A. J. Danner, B. Wang, S.-J. Chua, and J.-K. Hwang, "Fabrication of efficient light-emitting diodes with a self-assembled photonic crystal array of polystyrene nanoparticles," IEEE Photon. Technol. Lett. **20**, 48–50 (2008).
33. T. Prasad, R. Rengarajan, D. M. Mittleman, and V. L. Colvin, "Advanced photonic crystal architectures from colloidal self-assembly techniques," Opt. Mater. **27**, 1250–1254 (2005).
34. U. Gruning, V. Lehmann, and C. M. Engelhardt, "Two-dimensional infrared photonic band gap structure based on porous silicon," Appl. Phys. Lett. **66**, 3254–3256 (1995).
35. S. Rowson, A. Chelnokov, and J. M. Lourtioz, "Two-dimensional photonic crystals in macroporous silicon: from mid-infrared ($10\,\mu$m) to telecommunication wavelengths ($1.3–1.5\,\mu$m)," J. Lightwave Technol. **17**, 1989–1995 (1999).
36. A. Birner, A. P. Li, F. Mueller, U. Goesele, P. Kramper, V. Sandoghdar, J. Mlynek, K. Busch, and V. Lehmann, "Transmission of a microcavity structure in a two-dimensional photonic crystal based on macroporous silicon," Mater. Sci. Semicond. Process. **3**, 487–491 (2000).
37. T. Zijlstra, E. Van Der Drift, M. J. A. De Dood, E. Snoeks, and A. Polman, "Fabrication of two-dimensional photonic crystal waveguides for $1.5\,\mu$m in silicon by deep anisotropic dry etching," J. Vac. Sci. Technol. B **17**, 2734–2739 (1999).
38. M. Loncar, T. Doll, J. Vuckovic, and A. Scherer, "Design and fabrication of silicon photonic crystal optical waveguides," J. Lightwave Technol. **18**, 1402–1411 (2000).
39. A. Chelnokov, S. David, K. Wang, F. Marty, and J. M. Lourtioz, "Fabrication of 2-D and 3-D silicon photonic crystals by deep etching," IEEE J. Sel. Top. Quantum Electron. **8**, 919–927 (2002).
40. R. C. Rumpf and E. G. Johnson, "Fully three-dimensional modeling of the fabrication and behavior of photonic crystals formed by holographic lithography," J. Opt. Soc. Am. A **21**, 1703–1713 (2004).
41. V. Berger, O. Gauthier-Lafaye, and E. Costard, "Fabrication of a 2D photonic bandgap by a holographic method," Electron. Lett. **33**, 425–426 (1997).
42. M. Campbell, D. N. Sharp, M. T. Harrison, R. G. Denning, and A. J. Turberfield, "Fabrication of photonic crystals for the visible spectrum by holographic lithography," Nature **404**, 53–56 (2000).
43. L. Z. Cai, X. L. Yang, and Y. R. Wang, "All fourteen Bravais lattices can be formed by interference of four noncoplanar beams," Opt. Lett. **27**, 900–902 (2002).
44. L. Z. Cai, X. L. Yang, and Y. R. Wang, "Formation of three-dimensional periodic microstructures by interference of four noncoplanar beams," J. Opt. Soc. Am. A **19**, 2238–2244 (2002).
45. L. Z. Cai, X. L. Yang, and Y. R. Wang, "Formation of a microfiber bundle by interference of three noncoplanar beams," Opt. Lett. **26**, 1858–1860 (2001).
46. J. L. Stay and T. K. Gaylord, "Three-beam-interference lithography: contrast and crystallography," Appl. Opt. **47**, 3221–3230 (2008).
47. J. L. Stay and T. K. Gaylord, "Contrast in four-beam-interference lithography," Opt. Lett. **33**, 1434–1436 (2008).